Clim Dyn (2016) 47:1661–1672
DOI 10.1007/s00382-015-2926-1

Influence of altered low cloud parameterizations for seasonal variation of Arctic cloud amount on climate feedbacks

Yoojin Kim[1,2] · Yong-Sang Choi[2,5] · Baek-Min Kim[3] · Hyerim Kim[4]

Received: 9 July 2015 / Accepted: 19 November 2015 / Published online: 10 December 2015

Abstract This study investigates the alteration of climate feedbacks due to overestimated wintertime low-level cloud amount bias over the Arctic region (60°N–90°N) in a climate model. The climate feedback was quantitatively examined through radiative kernels that are pre-calculated radiative responses of climate variables to doubling of carbon dioxide concentration in NCAR Community Atmosphere Model version 3 (CAM3). Climate models have various annual cycle of the Arctic cloud amount at the low-level particularly with large uncertainty in winter and CAM3 may tend to overestimate the Arctic low-level cloud. In this study, the seasonal variation of low-level cloud amount was modified by reducing the wintertime cloud amount by up to 35 %, and then compared with the original without seasonal variation. Thus, we investigate how that bias may affect climate feedbacks and the projections of future Arctic warming. The results show that the decrease in low-level cloud amount slightly affected the radiation budgets because of a small amount of incident solar insolation in winter, but considerably changed water vapor and temperature profiles. Consequently, the most distinctive was decreases in water vapor feedback and contribution of heat transport (by -0.20 and -0.55 W m^{-2} K^{-1}, respectively) and increases in the lapse rate feedback and cloud feedback (by 0.13 and 0.58 W m^{-2} K^{-1}, respectively) during winter in this model experiment. This study suggests that the change in Arctic cloud amount effectively reforms the contributions of individual climate feedbacks to Arctic climate system and leads to opposing effects on different feedbacks, which cancel out in the model.

Keywords Climate model feedback · Radiative kernels · Arctic cloud parameterization

1 Introduction

The high-latitude regions are known to be highly sensitive to increasing greenhouse gas, mainly because of ice-albedo feedback (Screen and Simmonds 2010; Crook and Forster 2014) and/or the poleward heat transport (Alexeeve et al. 2005; Solomon 2006). However, recently it has been found that the lapse rate feedback was also a main contributor for sensitivity in Arctic region in dynamical model simulations (Pithan and Mauritsen 2014). Moreover, cloud feedback is an important source of Arctic amplification (Taylor et al. 2013), although cloud feedbacks provide the largest source of uncertainty of climate sensitivity (Soden and Held 2006). Such feedback processes in the Arctic region are indeed complicated, and their strengths require more clarification.

Climate feedbacks have been commonly quantified by the feedback parameters (λ) in the unit of watts per square meter per Kelvin, meaning the top-of-atmosphere (TOA) energy flux changes in the response to the surface temperature change. Because of the strong effect of Arctic clouds

✉ Yong-Sang Choi
ysc@ewha.ac.kr

1 Climate Research Department, APEC Climate Center, Busan, Republic of Korea

2 Department of Atmospheric Science and Engineering, Ewha Womans University, Seoul, Republic of Korea

3 Korea Polar Research Institute, Incheon, Republic of Korea

4 Department of Atmospheric Sciences, Yonsei University, Seoul, Republic of Korea

5 Department of Environmental Science and Engineering, Ewha Womans University, 52, Ewhayeodae-gil, Seodaemun-gu, Seoul 120-750, Republic of Korea

on the energy budget and the distributions of many climate variables such as cloud, water vapor, lapse rate, and surface albedo, the Arctic cloud simulation would be of vital importance in determining individual climate feedbacks. The Arctic cloud simulation is, however, a great challenge in current climate models. For example, different influences of cloud phase (ice and liquid) onto the net surface longwave radiation in the Arctic winter are difficult to be parameterized in climate models (Shupe and Intrieri 2004; Cesana et al. 2012a, b), and parameterization of ice nucleation processes in mixed-phase clouds is still insufficient to simulate the observation with climate models (Xie et al. 2013). In addition, reliable long-term observations of various cloud characterization in the Arctic region including height, thickness, optical depth, and types are insufficient to get insight of the cloud parameterization (Comiso and Hall 2014).

The seasonality is one of the important characteristics of Arctic cloud. Although there are large inter-satellite spreads of cloud observations (Chan and Comiso 2013), the satellite data generally show the minimum cloud amount in winter season. However, most climate models could not capture the seasonality (Liu et al. 2012; Vavrus and Waliser 2008). Vavrus and Waliser (2008) (hereafter VW08) simply replaced the Arctic low cloud parameterization to alleviate the overestimated cloud in freezing seasons. The VW08 altered the low-level cloud scheme by restriction of specific humidity during winter to make the more natural annual cycle of cloud amount in a model. We adapted the cloud amount function suggested by VW08, for the sake of altering seasonal cloud amount.

How Arctic climate feedbacks would be affected by the cloud amount change is a key question in this study. Quantitative calculation of the changes of the individual climate feedback parameters in the climate model is possible using the radiative kernels since they can allow one to convert the changes in individual climate variables into their radiative changes, pre-calculated by the radiative transfer modeling (e.g., Soden et al. 2008). Nonlinear interaction among individual feedbacks may not be well explained in this approach (Mauritsen et al. 2013). Nevertheless, this approach enables the calculation of the changes in the climate feedbacks, due to the modification of Arctic cloud amount. As the Arctic climate is characterized by a strong seasonal cycle, seasonally different solar radiation is an important characteristic in the Arctic climate system. Thus, seasonally different climate feedbacks were quantified in model experiments. Detailed model experiment design and methodology for calculating the climate feedbacks using the radiative kernels will be explained in the next section.

2 Methodology

2.1 Model description and experiment design

This study was performed with the Community Atmosphere Model version 3 (CAM3) developed by the National Center for Atmosphere Research (Collins et al. 2004). CAM3 remains useful to investigate the present question as to how cloud amount affects climate feedbacks as used by many recent studies (Jonko et al. 2012, 2013; Choi et al. 2014a). Community Land Model version 3 (CLM3) (Oleson et al. 2004) is embraced to simulate land surface and subsurface layers, whereas the Slab Ocean Model (SOM) and thermodynamic sea ice model were used to calculate the physical processes over ocean and sea ice, respectively. Flux coupler is the medium for heat and momentum fluxes between CAM3, CLM3, and SOM. Using the SOM, CAM3 reaches to the equilibrium climate state under CO_2 doubling, which is quite similar to that simulated using a full-depth ocean model in much shorter time (Kiehl et al. 2006; Danabasoglu and Gent 2009). The equilibrium climate sensitivity of CAM3, 2.7 °C, is a middle level among the third phase of the Coupled Model Intercomparison Project (CMIP3) (Meehl et al. 2007).

It should be noted that the cloud parameterization in the updated version of the model (CAM4 and CAM5) has been significantly changed (Neale et al. 2010). According to Kay et al. (2012), the evolution of modeled Arctic low cloud fraction is distinguished especially during winter time. Interestingly, Arctic low cloud fraction in CAM3 during winter time is more similar to that in CAM5, and rather differs from CAM4 (comparing the black lines in Fig. 1c with Fig. 11 of Kay et al. 2012). On the other hand, the equilibrium climate sensitivity of CAM4 is 3.2 K and that of CAM5 is 4.0 K (Gettelman et al. 2012). However, the change in the climate sensitivity is mainly attributed to the change in shortwave cloud feedback in 'the tropics and middle latitudes' (Gettelman et al. 2012), not to the Arctic climate feedbacks. Therefore, the Arctic climate feedbacks among different version of CAMs are comparatively stable than the other regions, despite of the large change of the low-level cloud fraction during winter time. The reason will be investigated in this study.

The cloud parameterization in CAM3 consists of convective and stratiform processes (Boville et al. 2006; Collins et al. 2006). The CAM3 low-level cloud amount function was calculated using the grid box-averaged relative humidity (RH):

$$f = \left[\frac{RH - RH_{Min}}{1 - RH_{Min}}\right]^2. \quad (1)$$

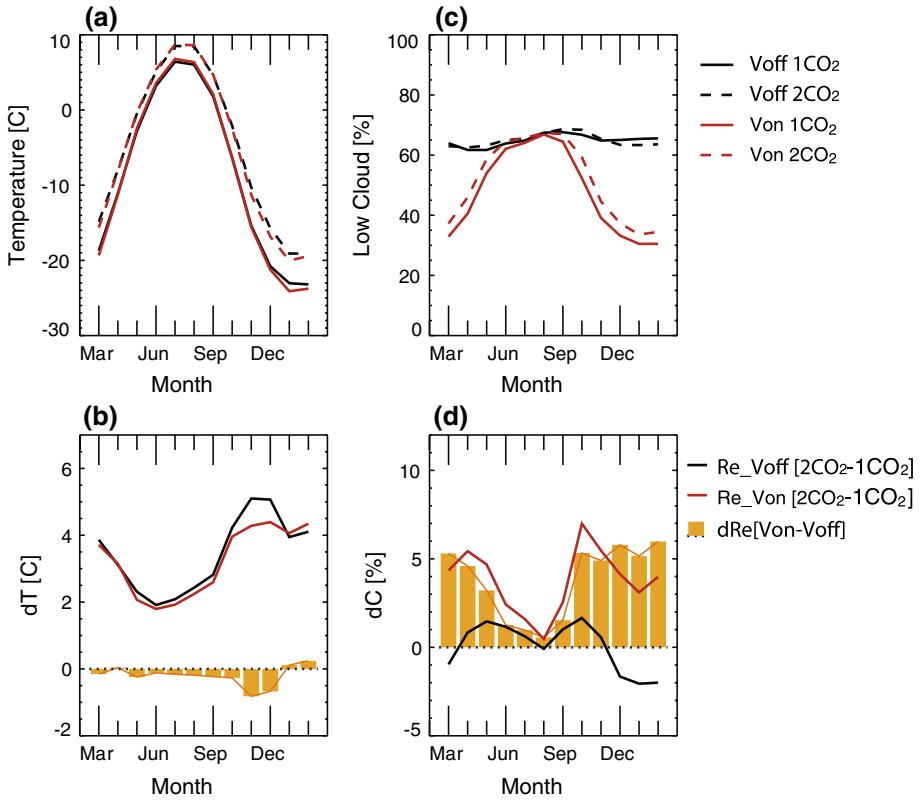

Fig. 1 Annual cycle of Arctic **a** surface temperature of C_Voff, D_Voff, C_Von and D_Von; **b** responses of surface temperature for Voff and Von experiments. Same annual cycle but for **c** low-level cloud amount and **d** responses of low-level cloud amount. Responses represent the differences of the temperature/cloud amount from the control to 2 × CO_2 condition in each cloud scheme experiment. The differences in the responses between the Voff and Von schemes are also plotted as *orange bars* in **b** and **d**. Last 40 years are averaged at each month over the Arctic region [60°N–90°N]

The RH_{Min} is the minimum RH at the level clouds are formed. However, this representation is not suitable for dry and extremely cold atmospheric condition of typical Arctic winter (Beesley 2000). VW08 implemented a threshold value (0.003 kg kg^{-1}) of specific humidity (q) to adjust the cloud fraction in the cold and dry atmospheric condition:

$$f = f\left[max\left(0.15, min\left(1.0, \frac{q}{0.003}\right)\right)\right]. \quad (2)$$

This formula effectively reduces the derived cloud fraction by Eq. (1) only where the q value falls below the threshold value, although it considers temperature and humidity only. Consequently, this reforms the seasonal cycle of cloud amount, and therefore reduces the bias in low-level stratiform cloud amount (750 hPa or higher) in the Arctic winter. Thus the alteration of cloud scheme is useful to examine the effect of seasonality of cloud although this does not promise the physical balance in the model world.

The two different cloud schemes, named as Voff and Von (original parameterization and replaced one respectively as in VW08) were tested in the simulations by CAM3. To calculate the equilibrium climate sensitivity for each cloud scheme, four 100-year simulations are conducted: two for the control concentration of CO_2 (C_Voff, C_Von) and two for the doubled concentration of CO_2 (D_Voff, D_Von). Last 40 model years for each simulation were analyzed to obtain an equilibrated climatology. The response of variables to 2 × CO_2 was measured as the difference between two equilibrated climatology (D_Voff minus C_Voff and D_Von minus C_Von). The control simulation, twentieth century CO_2 concentration is 355 ppmv, and the doubled CO_2 concentration is 710 ppmv. In addition, the ocean flux from the subsurface layer of the mixed layer in all experiments is prescribed to the same value as that of the Von control experiment. This constraint enables to obtain climate feedbacks largely associated with atmospheric responses to 2 × CO_2.

2.2 Calculation of climate feedbacks

The climate feedback parameter (λ) is defined as the changes in the radiative flux (dR) at the TOA in response to the change in the global (or regional) mean surface temperature ($d\bar{T}_s$), because of the increase in the CO_2 concentration from control to doubling. The imposed global radiative forcing (G) owing to the doubling of CO_2 is 3.36 W m^{-2} (y-axis intercept calculated by the regression of the net downward flux at TOA against the global average surface air temperature change for 40-year-run) (Gregory et al. 2004). Then, radiative flux is changed at TOA to balance the imposed forcing ($dR = -G$). The total climate feedback parameter (λ), total derivative ($dR/d\bar{T}_s$), can be separated into several partial derivatives with respect to different feedback processes using the chain rule as shown in the following equation:

$$\lambda = \frac{dR}{d\bar{T}_s} = \sum_i \frac{\partial R}{\partial x_i}\frac{dx_i}{d\bar{T}_s} \tag{3}$$

Here, different feedback processes in the last term in Eq. (3) indicate the change in the flux because of various variables, x_i [e.g., temperature (T), cloud (C), water vapor (w), and albedo (α)], responding to $d\bar{T}_s$. The climate feedback parameters (in units of $\mathrm{W\,m^{-2}\,K^{-1}}$) by the Planck function (P) and lapse rate (L) are calculated as

$$\lambda_P = \frac{\partial R}{\partial T_s}\frac{dT_s}{d\bar{T}_s} + \frac{\partial R}{\partial T}\frac{dT_s}{d\bar{T}_s}, \tag{4a}$$

$$\lambda_L = \frac{\partial R}{\partial T}\frac{dT}{d\bar{T}_s} - \frac{\partial R}{\partial T}\frac{dT_s}{d\bar{T}_s}. \tag{4b}$$

Here, the Planck response acts like the negative feedback associated with the temperature change dependent on thermal emission. The Planck feedback consists in the two parts: the changes in surface temperature feedback ($\frac{\partial R}{\partial T_s}\frac{dT_s}{d\bar{T}_s}$) and vertical atmospheric temperature feedback ($\frac{\partial R}{\partial T}\frac{dT_s}{d\bar{T}_s}$). The lapse rate feedback is also relevant to temperature, but for the changes in temperature difference between upper level and surface ($dT - dT_s$). The sum of Eqs. (4a) and (4b), $\lambda_P + \lambda_L$ is known as the temperature feedback (λ_T); first terms in both the equations are remained to compose the temperature feedback. Thus, the temperature feedback represents the longwave flux change by the vertical and surface temperature distribution. The water vapor and albedo are also well-known variables affecting radiative flux at TOA, and feedback to the surface temperature and the corresponding climate feedback parameter were calculated as

$$\lambda_w = \frac{\partial R}{\partial w}\frac{dw}{d\bar{T}_s}; \quad \lambda_\alpha = \frac{\partial R}{\partial \alpha}\frac{d\alpha}{d\bar{T}_s} \tag{4c}$$

where the partial derivatives ($\partial R/\partial x_i$) are the monthly radiative feedback kernels for CAM3 (Shell et al. 2008; Soden et al. 2008). The radiative kernels describe the radiative changes at TOA in response to the perturbation of variables (T, w, α) that affects radiative flux, and these are used in previous studies for computing and comparing individual feedback parameters (Shell et al. 2008; Jonko et al. 2012; Choi et al. 2014a).

The cloud feedback parameter (λ_C) is defined by using non-cloud variable kernels ($K_i = \partial R/\partial x_i$). The differences between clear-sky (K_i^0) and all-sky kernels (K_i) are used to estimate the effect of the cloud radiative feedback (Soden et al. 2008, Jonko et al. 2012, Shell et al. 2008):

$$\lambda_C = \frac{dC_{RF}}{d\bar{T}_s} + \left(K_T^0 - K_T\right)\left(\frac{dT}{d\bar{T}_s}\right) + \left(K_w^0 - K_w\right)\left(\frac{dw}{d\bar{T}_s}\right) + \left(K_\alpha^0 - K_\alpha\right)\left(\frac{d\alpha}{d\bar{T}_s}\right). \tag{4d}$$

The difference of cloud radiative forcing (dC_{RF}) between the doubled and control CO_2 world is calculated from the longwave and shortwave radiative changes by cloud in model.

The total feedback is the sum of Planck, lapse rate, cloud, water vapor, and albedo feedback parameters. Thus, the Eq. (3) can be rewritten as

$$\lambda = \lambda_P + \lambda_L + \lambda_C + \lambda_w + \lambda_\alpha + \lambda_{Res}. \tag{5}$$

Here the residual feedback parameter (λ_{Res}) mainly occurs from the atmospheric heat energy transport and uptake/release of heat flux from Arctic Ocean. And the nonlinearities of the radiative kernels also contribute the residual feedback parameter. Individual feedback parameters are functions of latitude, longitude, altitude (except for surface albedo and cloud feedback), and time. Thus, the feedback parameters are integrated from the surface to the tropopause and averaged globally or regionally and seasonally. The tropopause is simply defined to be 300 hPa at the pole and linearly decreased to 100 hPa at the equator (Soden and Held 2006; Jonko et al. 2012; Choi et al. 2014a).

The changes in the individual and total climate feedback parameters because of the VW08 scheme is designated by $\lambda' = \lambda'_P + \lambda'_L + \lambda'_C + \lambda'_w + \lambda'_\alpha + \lambda'_{Res}$, where primes are the Von minus Voff. Therefore, examining λ' is the main objective of this study. Hereafter, λ' on the annual, summer (June, July and August), and winter (December, January and February) averages for the Arctic region [60°N–90°N] will be investigated.

3 The impact of the cloud modification on climate feedbacks

3.1 Mean climate states

Prior to discuss climate feedbacks, the equilibrium climate states for control (C_Voff and C_Von) simulations are listed in Table 1. This table overall shows that the use of the cloud scheme (Von) actually changed winter low-level cloud amount without notable changes in the other climate variables (cloud radiative forcing, net radiative flux, sea ice fraction, and surface albedo). Because of the Von scheme, the annual low-level cloud amount decreased by 19 % (from 66 to 47 %) in control CO_2 simulation, and in addition the winter cloud amount decreased by 35 % (from 65 to 30 %) (a in Table 1). The two standard deviations (2σ) of the summer, winter, and annual-mean low-level cloud amounts are 0.03, 0.02, and 0.01 in Voff simulation, respectively. Here, we suppose that the significant change is beyond 2σ (95 % values of a Gaussian distribution). Contrary to the winter cloud, the summer cloud amount does not decrease significantly over the Arctic region. However,

Table 1 The Arctic [60°N–90°N] averages (40 years) of the climate variables for the Voff and Von experiments in control CO_2 concentrations (C_Voff and C_Von)

Variable	Season	C_Voff	C_Von	C_Von minus C_Voff
a				
Low-level cloud amount (air pressure ≥ 750 hPa)	Summer	0.67 (0.03)	0.66 (0.03)	−0.01
	Winter	0.65 (0.02)	0.30 (0.02)	−0.35
	Annual	0.66 (0.01)	0.47 (0.01)	−0.19
b				
Ts (K)	Summer	277.72 (0.68)	278.08 (0.62)	0.36
	Winter	249.38 (1.84)	248.65 (1.77)	−0.73
	Annual	263.42 (0.72)	263.27 (0.76)	−0.15
c				
Shortwave cloud radiative forcing (W/m^2)	Summer	−101.78	−101.39	0.39
	Winter	−1.61	−1.35	0.25
	Annual	−38.87	−38.04	0.83
d				
Shortwave net flux at TOA (downward) (W/m^2)	Summer	203.52	205.26	1.74
	Winter	7.10	7.38	0.28
	Annual	91.16	92.73	1.57
e				
Shortwave net flux at surface (downward) (W/m^2)	Summer	101.38	103.11	1.73
	Winter	2.69	3.03	0.34
	Annual	43.41	45.19	1.78
f				
High-level cloud amount (air pressure ≤ 750 hPa)	Summer	0.27	0.27	0.
	Winter	0.23	0.22	−0.01
	Annual	0.24	0.24	0.
g				
Longwave cloud radiative forcing (W/m^2)	Summer	25.65	25.64	−0.01
	Winter	16.85	15.81	−1.04
	Annual	21.50	20.65	−0.85
h				
Longwave net flux at TOA (upward) (W/m^2)	Summer	218.27	218.97	0.70
	Winter	165.60	166.37	0.77
	Annual	190.41	191.63	1.22
i				
Longwave net flux at surface (upward) (W/m^2)	Summer	31.62	32.29	0.67
	Winter	30.89	38.38	7.49
	Annual	31.90	37.44	5.54
j				
Latent heat flux at surface	Summer	25.35	26.04	0.69
	Winter	14.04	13.21	−0.83
	Annual	18.52	18.16	−0.36
k				
Sensible heat flux at surface	Summer	7.88	8.19	0.31
	Winter	7.17	1.27	−5.90
	Annual	8.06	4.69	−3.37
l				
Sea ice fraction	Summer	0.204	0.203	−0.001
	Winter	0.369	0.368	−0.001
	Annual	0.294	0.292	−0.002

Table 1 continued

Variable	Season	C_Voff	C_Von	C_Von minus C_Voff
m				
Surface albedo for diffuse radiation	Summer	0.362	0.357	−0.005
	Winter	0.495	0.495	0.
	Annual	0.483	0.480	−0.003

2-sigma values for seasonal-mean and annual-mean variables of low-level cloud and surface temperature are written in brackets

the impact of the cloud bias correction is low on the surface temperature. The Arctic temperature changes (0.36 and −0.73 K in the summer and winter, respectively) due to the Von scheme are less than the 2σ of the arctic temperature mean (0.68 and 1.84 K in the summer and winter, respectively) in the control simulation (b in Table 1). The change in the annual-mean surface temperature (−0.15 K) is even smaller.

Then why the surface temperature change is very small despite the large decrease of cloud amount? To answer this question, variables affecting the radiative forcing and therefore the temperature in the control CO_2 simulations are explained as the following. The decrease in the winter cloud amount is large; however, the effect on the shortwave radiative flux at TOA and surface is not so large because of small shortwave cloud radiative forcing in the Arctic winter (c, d and e in Table 1). The Von scheme only affected the low-level cloud with temperature closer to the surface temperature (a and f in Table 1). Thus, the cloud radiative forcing and thermal longwave radiative flux at TOA were not changed largely (g and h in Table 1). The change in the longwave net flux at the surface is large, but does not necessarily affect the surface temperature due to compensation of the surface turbulent heat fluxes (latent and sensible) (h i, j and k in Table 1). Moreover, sea ice cover and albedo changes are trivial (l and m in Table 1) because of the small change in the surface temperature (b in Table 1), resulting in a small change in the radiative flux at the surface and TOA (d, e, l, and m in Table 1).

To put it simply, the mean states of the major climate variables in the Voff and Von conditions are almost equal, although the cloud amount is largely different in winter. Thus, it can be said that the difference in the climate feedbacks between the Voff and Von conditions, which will be shown in the next section, may not be attributed to different mean climate states, but mainly to the effect of low-level cloud response to the 2 × CO_2 simulations.

3.2 Climate feedbacks

We shall begin with a discussion about the differences in the equilibrium climate states between the control and 2 × CO_2 simulations, in order to investigate the effect of the Von scheme on the individual and total climate feedbacks. The annual cycle for 40 years of the Arctic surface temperature and the response to 2 × CO_2 ($d\bar{T}_s = \bar{T}_{s,2CO_2} - \bar{T}_{s,1CO_2}$) are shown in Fig. 1a, b. The increases in the surface temperature because of 2 × CO_2 ($d\bar{T}_s$) were measured by the difference between the solid line ($\bar{T}_{s,1CO_2}$) and the dashed line ($\bar{T}_{s,2CO_2}$) in Fig. 1a both for Voff and Von simulations. The responses ($d\bar{T}_s$) for the Voff and Von schemes are plotted as the black and red lines in Fig. 1b, respectively, showing larger values in the winter than other seasons. The differences in the surface temperature responses between the Von and Voff experiments ($d\bar{T}'_s = (d\bar{T}_s)_{Von} - (d\bar{T}_s)_{Voff}$) are also plotted in Fig. 1b (orange bars), showing distinctively larger differences in November and December. On the annual average, $d\bar{T}_s$ in the Voff simulation is 3.5 K (the annual mean of the black line in Fig. 1b), whereas $d\bar{T}_s$ in the Von simulation is 3.27 K (the annual mean of the red line in Fig. 1b). Namely, the Von scheme makes the equilibrium climate sensitivity to 2 × CO_2 (the orange bars in Fig. 1b) decreased. However, the surface temperature change because of the use of the Von scheme only takes 6.6 % of the climate sensitivity to 2 × CO_2 (i.e., $d\bar{T}'_s/(d\bar{T}_s)_{Voff} = (3.27 - 3.5)/3.5$).

Figure 1c shows that the annual cycles of low-level cloud amount in the Voff (black lines) and Von simulations (red lines). The low-level cloud amount for the cold dry seasons was unrealistically large in the Voff simulation, but decreased in the Von simulation (VW08). The cloud responses to 2 × CO_2 ($d\bar{C} = \bar{C}_{2CO_2} - \bar{C}_{1CO_2}$) and their differences between the Von and Voff simulations ($d\bar{C}' = (d\bar{C})_{Von} - (d\bar{C})_{Voff}$) are also plotted in Fig. 1d, and $d\bar{C}'$ were amplified for most periods except the summer (the orange bars in Fig. 1d). $d\bar{C}$ for the Voff simulation is only 0.048 % on the annual average (the annual mean of the black line in Fig. 1d), whereas $d\bar{C}$ for the Von simulation is 3.8 % (the annual mean of the red line in Fig. 1d). Thus, the Von scheme increased cloud responses, $d\bar{C}$. The Von simulation (VW08) reduces cloud amount in cold dry season in the control CO_2 simulation and this might derive the increase in cloud amount in the doubled CO_2 simulation, which is not necessarily realistic. To sum up, the change in the surface temperature responses on the doubled

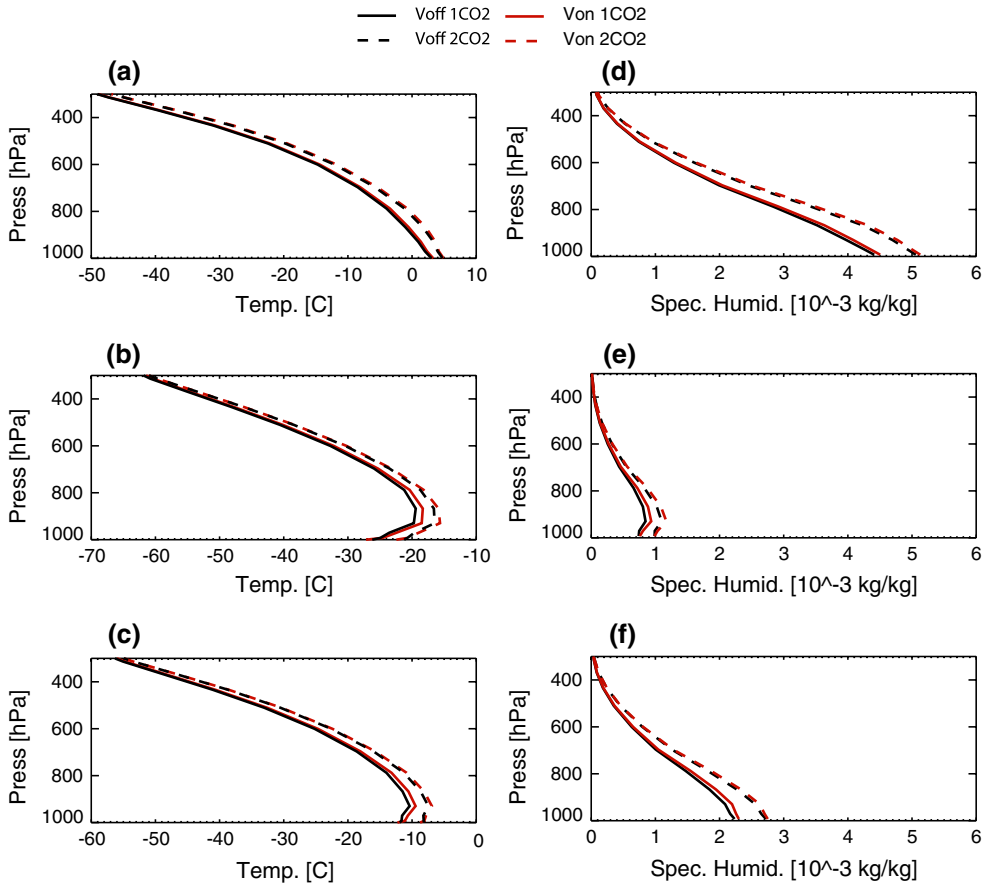

Fig. 2 Arctic [60°N–90°N] vertical temperature [°C] (*left*) and specific humidity [kg kg^{-1}] (*right*) profiles for **a**, **d** summer, **b**, **e** winter and **c**, **f** annual mean from 1000 hPa to 300 hPa. The last 40 years for each simulation, C_Voff, C_Von, D_Voff and D_Von are averaged. The tropopause is approximately at 300 hPa in the Arctic region, and temperature decreases as pressure decreases up to tropopause, but there is an inverse layer at the lower troposphere during winter

CO_2 due to the Von scheme is only 6.6 % in the control simulation, in spite of the large changes in cloud responses.

The vertical profiles of temperature for summer, winter and annual mean are plotted (Fig. 2a–c). In the control simulations, the Voff and Von experiments do not make a large difference in tropospheric temperature (black and red solid lines), as shown in the surface temperature in Table 1. Rather, temperature differences between doubling and control CO_2 experiments at each cloud scheme are large (differences between dashed and solid lines are large) in summer, winter and also in a whole year. The inversion layer at the lower troposphere in winter shows cold and stable atmospheric condition in the Arctic region, which affect the temperature feedback parameter. The strong inversion layer in polar night is a consequence of radiative cooling at the surface. Thus cloudy and cloud-free state can affect the stability of the boundary layer (Pithan et al. 2014). The surface radiative cooling is strong in the cloud-free state, enhancing the atmospheric stability. However, the Von schemes in this study do not show the stronger stable states at the low-level during winter in the control and doubling CO_2 experiments as expected in the real world (see Figure 2 in Pithan et al. 2014). It is currently poor to represent the temperature inversions and associated near-surface variables in other GCMs as well (Barton et al. 2014). The inversion layer is consequently related to the temperature feedback and the detailed characteristic of temperature feedback will be discussed later.

The vertical profiles of water vapor (Fig. 2d–f) also show similar changes with temperature profile under the tropopause; atmospheric warming derives the increase in atmospheric water vapor capacity. The altered low-level (750 hPa and higher) cloud amount scheme is adapted under the specific humidity threshold, 0.003 kg kg^{-1}, thus the cloud fraction in winter season is calculated with the altered scheme, but the summer cloud fraction is hardly modified. The specific humidity profiles are not directly affected by cloud schemes because the altered cloud scheme does not change the water vapor.

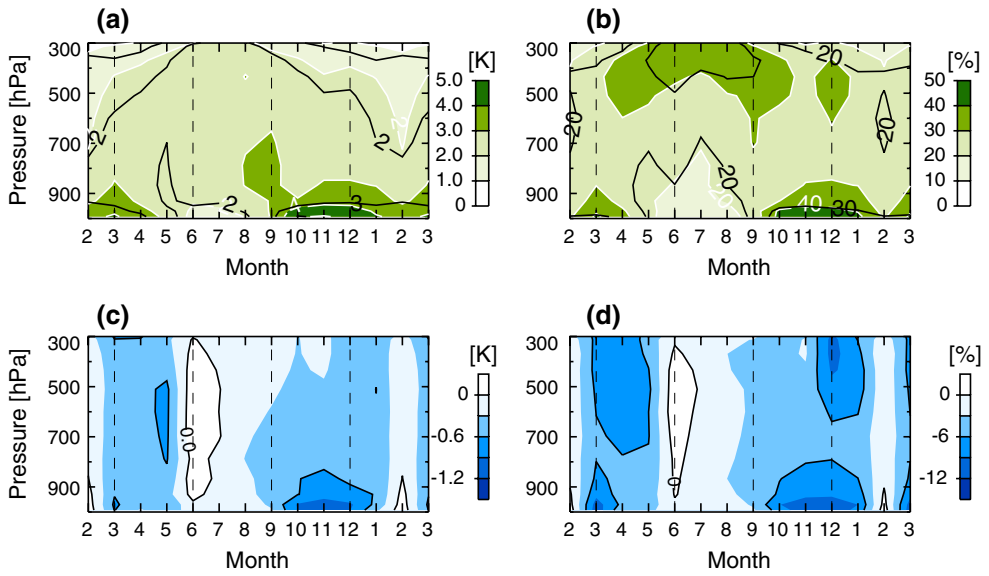

Fig. 3 Responses of **a** vertical temperature and **b** specific humidity to doubling of CO_2 condition for Voff (*shaded*) and Von (*black contour*) experiments at each month in the Arctic region [60°N–90°N]. For the specific humidity plot, the differences are expressed as a percent ((q(doubling) − q(control))/q(control)). Last 40 years are averaged. Response differences between the Voff and Von experiments for **c** temperature and **d** specific humidity are plotted at each month

The annual cycle of the vertical responses of the temperature and humidity to 2 × CO_2 are shown in Fig. 3. The temperature response to the 2 × CO_2 simulations was large at the low level in the cold seasons, which is consistent with the surface and atmospheric temperatures (Fig. 3a). Meanwhile, the responses of the water vapor due to the doubling CO_2 are closely related to the atmospheric warming during the cold season, because the air capacity for the humidity increases with increasing temperature.

The differences in the responses of temperature and humidity to 2 × CO_2 between the Von and Voff simulations are also shown in the low panel in Fig. 3c, d. These figures indicate that the Von scheme affects the temperature and humidity in the troposphere except the summer season. The cloud-free state can cause the surface cooling and enhance the inversion layer during winter in 2 × CO_2 simulations in spite of the poor representation of the inversion layer in the model comparing to those in observations. Thus, the Von scheme in this study shows less warming response at the surface due to the 2 × CO_2 simulations. The water vapor response shows similar characteristics to the temperature response because of their close relationship. These responses of vertical distributions of the temperature and humidity affect the climate feedbacks, in association with temperature, water vapor. Thus the climate feedback parameters are quantitatively calculated below.

The radiative kernels present the response of the TOA fluxes to the increased variables such as temperature, water vapor, and surface albedo. The vertical radiative kernels for Arctic temperature averaged over longitudes are displayed in Fig. 4a. The negative sign indicates that an increase in temperature increases the outgoing longwave radiation (i.e., decreases the net incoming radiation). Thus, Fig. 4a illustrates that the responses are relatively large in the upper level during warm seasons. Meanwhile, monthly surface temperature kernel distribution in Fig. 4b indicates that the responses are relatively large during winter at the surface.

The radiative kernels for water vapor are positive in Fig. 4c, meaning that an increase in water vapor is associated with an increase in the net radiation, for all levels in summer and high levels in the other seasons. This monthly vertical distribution is the sum of longwave and shortwave radiative kernels. While not shown in the figure, the slight negative values at lower levels during winter are due to the negative water vapor kernels of longwave radiation. The upper level is more sensitive to the perturbation of water vapor during late spring and summer than the lower level. The radiative kernel for albedo (Fig. 4d) gives the largest radiation quantity during the melting season, in spring and summer. A decrease in surface albedo derives an increase in incoming shortwave radiation and warming in that season. However, the surface albedo changes do not affect the radiation in the freezing season when the incoming shortwave radiation is negligible. The overall radiative responses to the increased variable is relatively large during spring or summer than the other seasons, while the opposite is true for the response to the increased surface temperature.

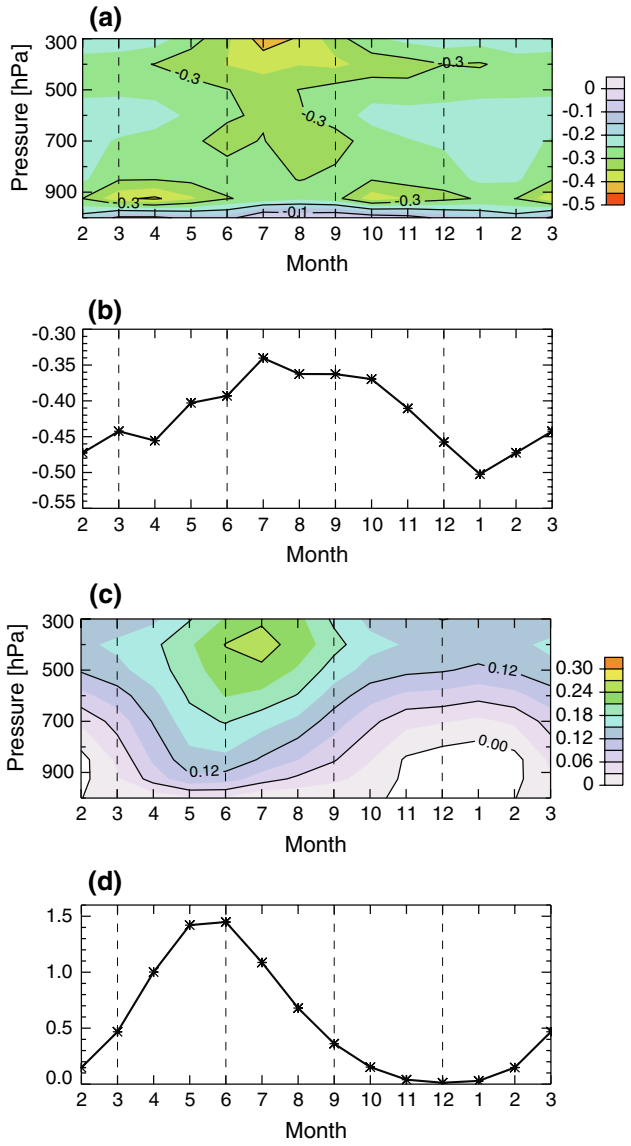

Fig. 4 The Arctic monthly distributions of **a** temperature kernel [W m^{-2} K^{-1}/100 hPa], **b** surface temperature kernel [W m^{-2} K^{-1}], **c** water vapor kernel [W m^{-2} K^{-1}/100 hPa], and **d** albedo kernel [W m^{-2}/ %]

The total and individual climate feedback parameters calculated from the radiative kernels, and Arctic surface temperature and net radiative response to imposed radiative forcing at TOA are listed in Table 2. The global total imposed radiative forcing at TOA is 3.36 W m^{-2} (Gregory et al. 2004) and surface temperature change is 2.1 °C in the 2 × CO_2 CAM3 model, so the total feedback parameter is −1.6 W m^2 K^{-1}, to balance the imposed radiative forcing at TOA. However, in terms of Arctic region, the surface temperature in the Arctic region is not the same as the global value, and transport of heat and energy should be considered in the regional aspect. Thus, the Arctic temperature changes are used to calculate the total and individual feedback parameters.

Among the individual annual feedback parameters, the Planck response (λ_P) is the largest contribution of outgoing radiative changes annually. The water vapor feedback (λ_w) is generally known to be positive in the globe annually for both longwave and shortwave radiation, because the water vapor uptakes radiation and warm the air. These are amplified in the tropical area and declined in the high-latitude regions.

Meanwhile, the seasonal variation of other individual feedback parameters is large because of the solar radiation and atmospheric vertical distribution. For example, the albedo feedback (λ_α) is concentrated in the summer, but small in the winter when the solar radiation is negligible. The lapse rate feedback (λ_L) is negative in the summer, but positive in the winter. The lapse rate feedback is generally negative over the globe. However, larger warming in the lower level is required to balance the radiative forcing in the Arctic region, where the atmosphere is stable in dry and cold conditions shown as the inversion layer in Fig. 2b. Thus the lapse rate feedback is positive during the winter (Pithan and Mauritsen 2014).

Interestingly, the cloud feedback (λ_C) also shows large seasonal variation in Voff simulation: negative during the summer and positive in the winter. Meanwhile, in the Von simulation, the cloud feedback is consistently positive. The Von simulation effectively reduces the low-level cloud during winter in the control simulation. This condition makes rooms for an increase in cloud amount responding to the doubling CO_2 properly in the model. Consequently, the cloud feedback responding to doubling CO_2 in Von simulation increases during winter owing to the longwave radiative forcing of cloud.

The residuals of kernel radiative forcing include discrepancies between the real and model world induced by the nonlinearities of radiative kernels of each variable and transport of atmospheric heat energy from other region. In addition, the substantial seasonal heat uptake and release of the Arctic oceans are also part of the residual. We assume the linearity of kernels, so that the residuals almost come from the heat energy of atmospheric transport and Arctic oceans in the model world. The negative residuals in the summer and annual mean in the Arctic region indicate the cooling effect by the heat loss. In the winter, the Voff simulation shows the positive residuals, implying the warming effect by the heat gain; however, the Von simulation shows the negative residuals, implying the cooling effect by the heat loss.

The VW08 scheme alters the climate feedbacks by ~7.3 % in the global warming simulation annually (λ'/λ). Even though the cloud fraction shows large decrease in the winter, the total feedback parameter (λ) alters by only

Table 2 The Arctic [60°N–90°N] averages of response of surface temperature ($d\bar{T}_s$), and climate feedback changes (λ), response to CO_2 doubling increases in Voff and Von experiments for 40 years (D_Voff-C_Voff and D_Von-C_Von)

Voff	$d\bar{T}_s$	λ	λ_P	λ_L	λ_w	λ_α	λ_C	λ_{Res}
Summer	2.09	−1.61	−2.73	−0.57	1.13	2.56	2.48	−4.48
Winter	4.48	−0.75	−2.5	0.95	0.96	0	−0.33	0.16
Annual	3.50	−0.96	−2.6	0.67	0.91	0.37	0.86	−1.18
Von	$d\bar{T}_s$	λ	λ_P	λ_L	λ_w	λ_α	λ_C	λ_{Res}
Summer	1.94	−1.73	−2.73	−0.7	1.17	2.56	2.64	−4.67
Winter	4.33	−0.78	−2.49	1.08	0.76	0	0.25	−0.37
Annual	3.27	−1.03	−2.6	0.77	0.89	0.37	1.03	−1.49

Difference (Von − Voff)	$d\bar{T}'_s$	λ'	λ'_P	λ'_L	λ'_w	λ'_α	λ'_C	λ'_{Res}
Summer	−0.15	−0.12	0	−0.13	0.04	0	0.16	−0.19
Winter	−0.15	−0.03	0.01	0.13	−0.20	0	0.58	−0.55
Annual	−0.23	−0.07	0	0.10	−0.02	0	0.17	−0.31
Comment		Total	Planck	Lapse rate	Water vapor	Surface albedo	Cloud	Residual
Difference proportion for annual	$6.6\,\frac{abs(d\bar{T}'_s)}{(d\bar{T}_s)_{Voff}}$	$7.3\,\frac{abs(\lambda')}{(\lambda)_{Voff}}$						

-0.03 W m^{-2} K^{-1} in the same season and -0.07 W m^{-2} K^{-1} in annual mean. Large increases in the cloud feedback ($\lambda'_C = 0.58$ W m^{-2} K^{-1}) and lapse rate feedback ($\lambda'_L = 0.13$ W m^{-2} K^{-1}) occur in the winter, but are compensated by the decrease in the energy transport ($\lambda'_{Res} = -0.55$ W m^{-2} K^{-1}) and water vapor feedback ($\lambda'_w = -0.2$ W m^{-2} K^{-1}) in the same season. The large increase in the cloud feedback is mostly canceled out by less heat transport during winter. This results from the alteration in the temperature and humidity vertical distributions at the low level during winter because of the VW08 scheme.

Meanwhile, in the summer, the total climate feedback parameter (λ) decreased by -0.12 W m^{-2} K^{-1} due to the VW08 scheme. This is due to the decreases in the lapse rate feedback ($\lambda'_L = -0.13$ W m^{-2} K^{-1}) and the heat transport ($\lambda'_{Res} = -0.19$ W m^{-2} K^{-1}), and due to their compensation by the increases in the water vapor feedback ($\lambda'_w = 0.04$ W m^{-2} K^{-1}) and cloud feedback ($\lambda'_C = 0.16$ W m^{-2} K^{-1}). After all, in the annual mean, the increases in the cloud feedback ($\lambda'_C = 0.17$ W m^{-2} K^{-1}) and lapse rate feedback ($\lambda'_L = 0.13$ W m^{-2} K^{-1}) almost offset the decreases in the heat transport ($\lambda'_{Res} = -0.31$ W m^{-2} K^{-1}) and water vapor feedback ($\lambda'_w = -0.02$ W m^{-2} K^{-1}). Thus a slight negative total feedback ($\lambda' = -0.07$ W m^{-2} K^{-1}) is induced.

The changes in the individual climate feedbacks by the Von scheme are considerably large in the model simulations. However, the total climate feedback parameter (λ) is certainly decreased slightly, although the overestimated low-level cloud in the model is decreased to resemble the observation data during the winter. Therefore, it cannot be said that the low-level winter cloud bias in the Arctic region has affected the overall future climate projection. However, the modification of the low-level winter clouds does reform the individual climate feedbacks in the model.

4 Conclusion and discussion

The influence of the changes in the seasonal cycle of the cloud fraction was investigated by the VW08 cloud scheme. This VW08 scheme alleviates the overestimated cloud fraction in the lower troposphere during the winter. This results in the decreases in the water vapor feedback (λ_w) and heat energy transport feedback (λ_{Res}), and the increases in the cloud feedback (λ_C) and lapse rate feedback (λ_L) in the same season. In the annual-mean, VW08 scheme acts similar to the winter: feedback parameters increase due to the lapse rate (λ_L) and cloud (λ_C), and decrease due to the water vapor (λ_w) and heat energy transport (λ_{Res}). Consequently, the VW08 scheme yielded a small decrease in the equilibrium surface temperature and total feedback parameter (λ) annually in the model under $2 \times CO_2$. It is important to note that the Arctic cloud affects not only the cloud feedback (λ_C), but also other climate feedbacks.

These experiments were performed with the CAM3 model, and the climate feedback strengths were calculated using CAM3 radiative kernels provided by Soden et al. (2008). Of course, the estimated climate feedback parameters and radiative kernels are dependent on the experimental settings and dynamics of the model. To examine the climate feedbacks of nature, the recent satellite observation study by Choi et al. (2014b) revealed that the

state-of-the-art climate models tend to underestimate the leading role of cloud in the ice-albedo feedbacks during the melting season, indicating that the physical processes associated with albedo feedback, should be further improved to connect clouds in the current models. Therefore, it should be borne in mind that the control albedo feedback parameter and their small change in this study are obtained from simulations from a single model. Confirming the result using other models would be desirable.

The climate feedback strengths calculated in this study are useful to investigate the contributions of seasonal cloud amount to the total climate feedback for a given region and season. Boisvert and Stroeve (2015) found from the Atmospheric Infrared Sounder that the increase in Arctic cloud amount in February and November is large during 2003–2013. This would eventually affect Arctic climate feedbacks as discussed throughout this paper. However, one should note that the climate feedback strengths confined in the Arctic region cannot be directly compared to those in the globe, because the feedback-related physical processes are not isolated in a regional scale. Crook et al. (2011) documented that the impact of Arctic climate feedback changes on the globe might be small, but can influence the meridional heating response. How the Arctic climate feedback changes by cloud changes actually affect the global climate is a subject of the future study.

Acknowledgments This work was supported by "Development of Geostationary Meteorological Satellite Ground Segment" program funded by NMSC (National Meteorological Satellite Centre) of KMA (Korea Meteorological Administration). Yoojin Kim acknowledges support from the APEC Climate Center. Baek-Min Kim was supported by Korea Meteorological Administration Research and Development Program (KMIPA2015-2093, PN15040). The radiative kernels for this paper are available at K. M. Shell's homepage (http://people.oregonstate.edu/~shellk/kernel.html). Kernel files: kernels.zip.

References

Alexeeve VA, Langen PL, Bates JR (2005) Polar amplification of surface warming on an aqua planet in "ghost forcing" experiments without sea ice feedbacks. Clim Dyn 24:655–666. doi:10.1007/s00382-005-0018-3

Barton NP, Klein SA, Boyle JS (2014) On the contribution of longwave radiation to global climate model biases in Arctic lower tropospheric statiblity. J Clim 27:7250–7269

Beesley JA (2000) Estimating the effect of clouds on the Arctic surface energy budget. J Geophys Res Atmos 105:10103–10117. doi:10.1029/2000JD900043

Boisvert LN, Stroeve JC (2015) AIRS satellite data reveal the Arctic is becoming warmer and wetter. Geophys Res Lett 42:4439–4446. doi:10.1002/2015GL063775

Boville BA, Rasch PJ, Hack JJ, McCaa JR (2006) Representation of clouds and precipitation processes in the Community Atmosphere Model version 3 (CAM3). J Clim 19:2184–2198. doi:10.1175/JCLI3749.1

Cesana G, Kay JE, Chepfer H, English JM, Boer G (2012a) New observations and climate model constraints from CALIPSO-GOCCP. Geophy Res Lett 39:L20804. doi:10.1029/2012gl053385

Cesana G, Kay JE, Chepfer H, English JM, Boer G (2012b) Ubiquitous low-level liquid-containing Arctic clouds: new observations and climate model constraints from CALIPSO-GOCCP. Geophys Res Lett 39:L20804. doi:10.1029/2012gl053385

Chan MA, Comiso JC (2013) Arctic cloud characteristics as derived from MODIS, CALIPSO, and CloudSat. J Clim 26:3285–3306

Choi Y-S, Ho C-H, Park C-E, Storelvmo T, Tan I (2014a) Influence of cloud phase composition on climate feedbacks. J Geophys Res Atmos 119:3687–3700. doi:10.1002/2013JD020582

Choi Y-S, Kim B-M, Hur S-K, Kim S-J, Kim J-H, Ho C-H (2014b) Connecting early summer cloud-controlled sunlight and late summer sea ice in the Arctic. J Geophys Res Atmos 119:11087–11099. doi:10.1002/2014JD022013

Collins WD et al (2004) Description of the NCAR Community Atmosphere Model (CAM 3.0). NCAR tech note. NCAR/TN-464 + STR. National Center for Atmospheric Research, Boulder, Colorado, USA

Collins WD, Rasch PJ, Boville BA, Hack JJ, McCaa JR, Williamson DL, Briegleb BP, Bitz CM, Lin S-J, Zhang M (2006) The formulation and atmospheric simulation of the Community Atmosphere Model version 3 (CAM3). J Clim 19:2144–2161. doi:10.1175/JCLI3760.1

Comiso JC, Hall DK (2014) Climate trends in the Arctic as observed from space. WIREs Clim Change 5:389–409. doi:10.1002/wcc.277

Crook JA, Forster PM (2014) Comparison of surface albedo feedback in climate models and observations. Geophys Res Lett 41:1717–1723. doi:10.1002/2014GL059280

Crook JA, Forster PM, Stuber N (2011) Spatial patterns of modeled climate feedback and contributions to temperature response and polar amplification. J Clim 24(14):3575–3592. doi:10.1175/2011JCLI3863.1

Danabasoglu G, Gent PR (2009) Equilibrium climate sensitivity: is it accurate to use a slab ocean model? J Clim 22:2494–2499. doi:10.1175/2008JCLI2596.1

Gettelman A, Kay JE, Shell KM (2012) The evolution of climate sensitivity and climate feedbacks in the community atmosphere model. J Clim 25:1453–1469

Gregory JM, Ingram WJ, Palmer MA, Jones GS, Stott PA, Thorpe RB, Lowe JA, Johns TC, Williams KD (2004) A new method for diagnosing radiative forcing and climate sensitivity. Gophys Res Lett 31:L03205. doi:10.1029/2003GL018747

Jonko AK, Shell KM, Sanderson BM, Danabasoglu G (2012) Climate feedbacks in CCSM3 under changing CO2 forcing. Part I: adapting the linear radiative kernel technique to feedback calculations for a broad range of forcings. J Clim 25:5260–5272. doi:10.1175/JCLI-D-11-00524.1

Jonko AK, Shell KM, Sanderson BM, Danabasoglu G (2013) Climate feedbacks in CCSM3 under changing CO2 forcing. Part II: variation of climate feedbacks and sensitivity with forcing. J Clim 26:2784–2795. doi:10.1175/JCLI-D-12-00479.1

Kay JE et al (2012) Exposing global cloud biases in the Community Atmosphere Model (CAM) using satellite observation and their corresponding instrument simulators. J Clim 25:5190–5207. doi:10.1175/JCLI-D-11-00469.1

Kiehl JT, Shields CA, Hack JJ, Collins WD (2006) The climate sensitivity of the Community Climate System Model version 3 (CCSM3). J Clim 19:2584–2596. doi:10.1175/JCLI4747.1

Liu Y, Key JR, Ackerman SA, Mace GG, Zhang Q (2012) Arctic cloud macrophysical characteristics from CloudSat and CALIPSO. Remote Sens Environ 124:159–173. doi:10.1016/j.rse.2012.05.006

Mauritsen T, Graversen RG, Klocke D, Langen PL, Stevens B, Tomassini L (2013) Climate feedback efficiency and synergy. Clim Dyn 41:2539–2554. doi:10.1007/s00382-013-1808-7

Meehl GA et al (2007) Global climate projections, in Climate Change 2007: the physical science basis. In: Solomon S et al (eds) Contribution of Working Group I to the Fourth Assessment Report of the Intergovernmental Panel on Climate Change. Cambridge University Press, Cambridge, pp 749–845

Neale RB et al (2010) Description of the NCAR Community Atmosphere Model (CAM 5.0). Technical note 486 + STR. National Center for Atmospheric Research, Boulder, Colorado, USA

Oleson KW et al (2004) Technical description of the Community Land Model (CLM). NCAR tech. note, NCAR/TN-461 + STR, National Center for Atmospheric Research, Boulder, Colorado, USA

Pithan F, Mauritsen T (2014) Arctic amplification dominated by temperature feedbacks in contemporary climate models. Nat Geosci 7:181–184. doi:10.1038/ngeo2071

Pithan F, Medeiros B, Mauritsen T (2014) Mixed-phase clouds cause climate model biases in Arctic wintertime temperature inversions. Clim Dyn 43:289–303. doi:10.1007/s00382-013-1964-9

Screen JA, Simmonds I (2010) The central role of diminishing sea ice in recent Arctic temperature amplification. Nature 464:1334–1337. doi:10.1038/nature09051

Shell KM, Kiehl JT, Shields CA (2008) Using the radiative kernel technique to calculate climate feedbacks in NCAR's community atmospheric model. J Clim 21:2269–2282. doi:10.1175/2007JCLI2044.1

Shupe MD, Intrieri JM (2004) Cloud radiative forcing of the Arctic surface: the influence of cloud properties, surface albedo, and solar zenith angle. J Clim 17:616–628

Soden BJ, Held IM (2006) An assessment of climate feedbacks in coupled ocean-atmosphere models. J Clim 19:3354–3360. doi:10.1175/JCLI3799.1

Soden BJ, Held IM, Colman R, Shell KM, Kiehl JT, Shields CA (2008) Quantifying climate feedbacks using radiative kernels. J Clim 21:3504–3520. doi:10.1175/2007JCLI2110.1

Solomon A (2006) The impact of latent heat release on polar climate. Geophys Res Lett 33:L07716. doi:10.1029/2005GL025607

Taylor PC, Cai M, Hu A, Meehl J, Washington W, Zhang GJ (2013) A decomposition of feedback contributions to polar warming amplification. J Clim 26:7023–7043. doi:10.1175/JCLI-D-12-00696.1

Vavrus S, Waliser D (2008) An improved parameterization for simulating Arctic cloud amount in the CCSM3 climate model. J Clim 21:5673–5687. doi:10.1175/2008JCLI2299.1

Xie S, Liu X, Zhao C, Zhang Y (2013) Sensitivity of CAM5-simulated Arctic clouds and radiation to ice nucleation parameterization. J Clim 26:5981–5999. doi:10.1175/JCLI-D-12-00517.1